Signature of collective elastic glass physics in surface-induced long-range tails in dynamical gradients

Asieh Ghanekarade¹, Anh D, Phan*², Kenneth S. Schweizer*³, David S. Simmons*¹

Author Affiliations: ¹Department of Chemical, Biological and Materials Engineering, University of South Florida, Tampa, FL, 33620, USA. ²Faculty of Materials Science and Engineering, Phenikaa University, Hanoi, Vietnam. ³Departments of Materials Science and Chemistry and Materials Research Laboratory, University of Illinois, Urbana, IL 61801, USA

Corresponding author contact information:

David S. Simmons: <u>dssimmons@usf.edu</u>

Kenneth S. Schweizer: kschweiz@illinois.edu

Anh D. Phan: anh.phanduc@phenikaa-uni.edu.vn

Abstract: Understanding the underlying nature of dynamical correlations believed to drive the bulk glass transition is a long-standing problem. Here we show that the form of spatial gradients of the glass transition temperature and structural relaxation time near an interface indeed provide signatures of the nature of relaxation in bulk glass forming liquids. We report results of long-time, large-system molecular dynamics simulations of thick glass-forming polymer films with one vapor interface, supported on a dynamically neutral substrate. We find that gradients in the glass transition temperature and logarithm of the structural relaxation time nucleated at a vapor interface exhibit two distinct regimes: a mediumranged, large amplitude exponential gradient, followed by a long-range slowly decaying tail that can be described by an inverse power law. This behavior disagrees with multiple proposed theories of glassy dynamics but is predicted by the Elastically Collective Nonlinear Langevin Equation theory as a consequence of two coupled mechanisms: a medium-ranged interface-nucleated gradient of surface modified local caging constraints, and an interfacial truncation of a long-ranged collective elastic field. These findings support a coupled spatially local-nonlocal mechanism of activated glassy relaxation and kinetic vitrification in both the isotropic bulk and in broken symmetry films.

Manuscript text: The underlying mechanism driving the experimentally observed kinetic glass transition has been one of the most enduring and debated open questions in condensed matter physics^{1,2}. The challenge is to explain the rapid growth upon cooling of the activation energy for structural (alpha) relaxation in "fragile" glass-forming liquids. Numerous theories have been proposed for this phenomenon¹. Most differ fundamentally in terms of the structural, thermodynamic, or dynamic property and physical mechanism postulated to drive the growth of the apparent activation energy. Proposed origins include loss of configurational entropy^{4–6}, loss of available free volume⁷, percolation of slow-relaxing domains⁸, dynamical facilitation among a small subset of mobile particles⁹, emergence of glassy elasticity on cooling¹⁰, onset of particle localization¹¹, and a coupled combination of long-range elasticity and cage scale localization^{12,13} both causally controlled by structural correlations. The core challenge of the field has been an inability to definitively discriminate between these various theoretical approaches.

Considerable research for 35 years has sought to employ confinement and broken symmetry in thin films and near interfaces to reveal the physics of dynamical cooperativity and thus to potentially resolve the nature of the bulk glass transition^{14–17}. Moreover, activated spatially heterogeneous dynamics near interfaces and under confinement is of high fundamental interest in its own right (e.g., for surface

diffusion¹⁸ and ultra-stable glass formation¹⁹), and it bears on the behavior of the wide range of materials that have internal or external dimensions on the nanoscale²⁰ including films²¹, nanocomposites²², block copolymers²³, semicrystalline materials²⁴, liquids in pores²⁵, and many more. It is now established that confinement and proximity to an interface can strongly modify the dynamics of glass-forming liquids, over a considerably longer distance than interfacial or confinement-induced perturbations to thermodynamics and structure^{16,17,21,26–28}. A challenge thus far has been a lack of sufficient knowledge of the spatially-resolved form of these alterations to definitively distinguish between proposed mechanisms of bulk glass formation and their alteration near interfaces. As reviewed recently²⁶, specific and distinct predictions of the spatial form of such gradients have been made by competing theories of glassy activated dynamics, including the Random First Order Transition (RFOT) entropy crisis theory²⁹, free volume percolation theories^{8,30}, the cooperative free volume model³¹, dynamical 'string' theories based on the Adams-Gibbs model³², and the Elastically Cooperative Nonlinear Langevin Equation (ECNLE) theory³³. The form of interfacial gradients in Tg and relaxation time thus appears to offer an opportunity to genuinely distinguish between competing theories of the glass transition.

Accordingly, here we perform long-time, large-system molecular dynamics simulations of a bead-spring polymer thin film supported on a dynamically neutral substrate, in order to elucidate the spatial form of the glass transition temperature (Tg) and structural relaxation time gradients out to large distances from a free vapor surface. Our exploration of the long-range nature of this gradient is motivated by recent predictions of ECNLE theory, which is a microscopic, force-based, particle-level theory for activated dynamics in (originally bulk) glass-forming liquids^{12,13}. In both the bulk and near interfaces, ECNLE theory predicts two additive and physically distinct, but intimately coupled, contributions to the total activation barrier ($F_{tot} = F_B + F_{el}$): a local cage scale barrier (F_B) associated with large amplitude particle hopping, and a longer-range collective elastic barrier (F_{el}) associated with the need for facilitating small amplitude elastic dilational displacements of all particles outside the cage to allow particle hopping. Recent ECNLE theory calculations for dynamical gradients near free surfaces have predicted that the near-field Tg gradient decays in an exponential manner as a function of distance (z) from the surface, but at large enough z decays as a scale-free inverse power law $(^{2}-^{1})^{33}$. The latter is a direct signature of the importance of collective elasticity for structural relaxation, with ECNLE theory predicting that the elastic barrier becomes increasingly dominant relative to its local cage analog upon cooling to Tg12,13. This power law tail decay form is a unique prediction, which if validated would provide new support for the idea that structural relaxation is of a coupled local-nonlocal character. After reporting our new simulation results, we quantitatively compare the data with a new asymptotic analytic ECNLE theory analysis and higherprecision numerical calculations for the spatial form of the Tg and alpha time gradients.

In Figure 1a, we report the simulated normalized glass transition temperature shift gradient as a function of distance z from the free surface of the film, where T_g is defined on a computational relaxation timescale of $10^5 \tau_{LI}$ (about 100 ns) based on purely in-equilibrium relaxation data (see Figure S2 in the SI for the underlying relaxation time temperature dependences). As can be seen in Figure 1a, the near-surface T_g gradient obeys an exponential form over the first 8-10 σ (nm) from the free surface, consistent with prior simulation studies of dynamics near vapor surfaces^{26,34–36}. However, beyond $z^{\sim}10\sigma$, the gradient transitions to a long-range tail that has not previously been reported in simulation or experiment. Large-z upward deviations from the exponential decay are well beyond uncertainty (propagated from standard deviations over 3 film and 3 bulk runs) and are qualitatively robust to the choice of relaxation time versus temperature fitting form and timescale convention employed to extract T_g (see Figures S3 and S4 in the

SI). Moreover, since the film data are normalized by data from very large bulk simulations, the large-z tail behavior cannot be an anomaly of normalization against a quantity that encodes a residual interface effect. Figure 1a illustrates that the long-range tail of the Tg gradient can be described as a power law with a slope of -1, although other slowly-decaying empirical descriptions are likely possible given the z-range of available data (which pushes the limit of current simulation capabilities) and their confidence intervals.

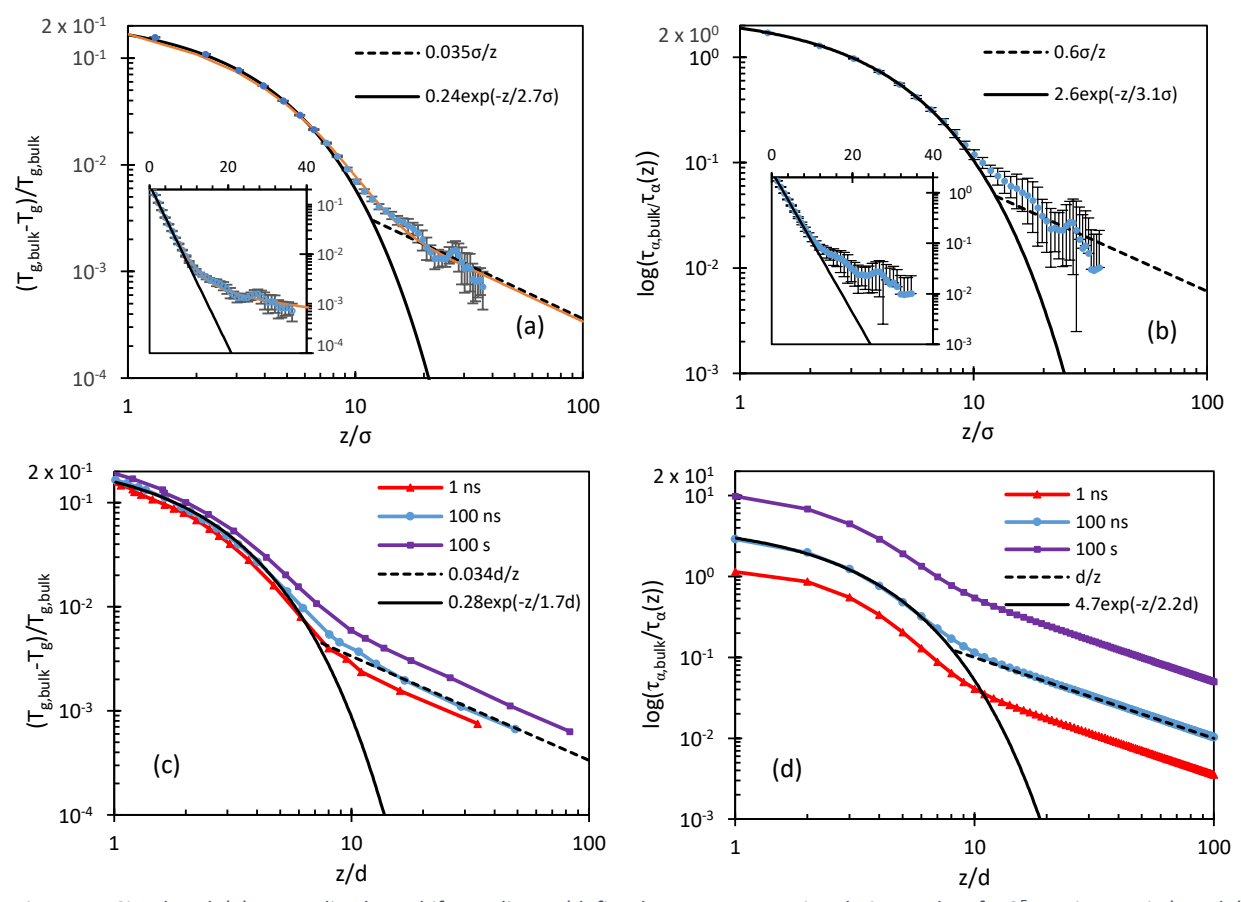


Figure 1. Simulated (a) normalized T_g shift gradients (defined at a computational timescale of 10^5 \Box time units) and (b) $\log(\tau_{\alpha,\text{bulk}}/\tau_{\alpha}(z))$ gradients (obtained at a temperature for which the bulk relaxation time is 10^5 \Box time units, using the form of Schmidtke et al.⁴⁰ to smooth data across multiple temperatures) vs normalized distance z/σ from the free surface. Data are presented as mean values with error bars reflecting standard deviations propagated from data for 3 films and 3 bulk runs. Solid black lines are fits of low-z data to a decaying exponential. Dashed black line is an inverse power law, z^{-1} . Solid orange curve in panel (a) is a fit to equation (6). Insets show the same data for a linear ordinate axis. ECNLE theory predictions for a spherical particle model (diameter, d) of (c) T_g gradients and (d) $\log(\tau_{\alpha,\text{bulk}}/\tau_{\alpha}(z))$ gradients plotted on logarithmic scales vs normalized distance z/d from the interface. Distinct data sets are results at very different choices of the vitrification timescale, as shown in the legends, and lines are exponential and power law fits to theory results in the low and high z limits, respectively, as shown in the legends.

As can be seen in Figure S5 in the SI, results for the alpha relaxation time gradient in $\tau_{\alpha,bulk}/\tau_{\alpha}(z)$ also exhibit a 2-regime form: a *double*-exponential form dominates for $z < 10~\sigma$ (consistent with prior simulation and experimental findings over this length scale range ^{18,26,37–39}), followed by a longer-ranged tail. The form of this tail is further clarified by fitting ⁴⁰ to data at multiple temperatures to obtain a reduced-noise calculation of the relaxation time at low temperature. As seen in Figure 1b, the long-range tail of $\log(\tau_{\alpha,bulk}/\tau_{\alpha}(z))$ can likewise be described by an inverse power law of essentially an identical form as found for the T_g gradient.

These simulation data are inconsistent with the gradient forms predicted by multiple theories of glass formation. RFOT predicts that the difference between the film and bulk relaxation rates decays exponentially with distance from the surface²⁹; this conflicts with the low-z regime, where empirically the relaxation time decays in a double-exponential manner. RFOT also does not predict any long-range tail, and, as shown in Figure S6, a multi-parameter fit of its predicted dynamic gradient form²⁹ does not qualitatively describe the simulation data in either regime. The cooperative free volume theory – a very different model – predicts a similar exponential relaxation time gradient³¹ that does not agree with either regime observed in simulation. Alternative phenomenological free-volume based slow domain percolation models predict a purely power-law T_g gradient⁸ and do not qualitatively capture the short-ranged exponential decay that quantitatively dominates surface behavior. the near The phenomenological "cooperative string" theory predicts a roughly double exponential decay of relaxation times but does not capture the longrange power law tail³². Broadly, the far field gradient appears to be qualitatively inconsistent with theories based on a static or dynamic length-scale that is cut off by a boundary in a critical phenomena spirit. This observation is

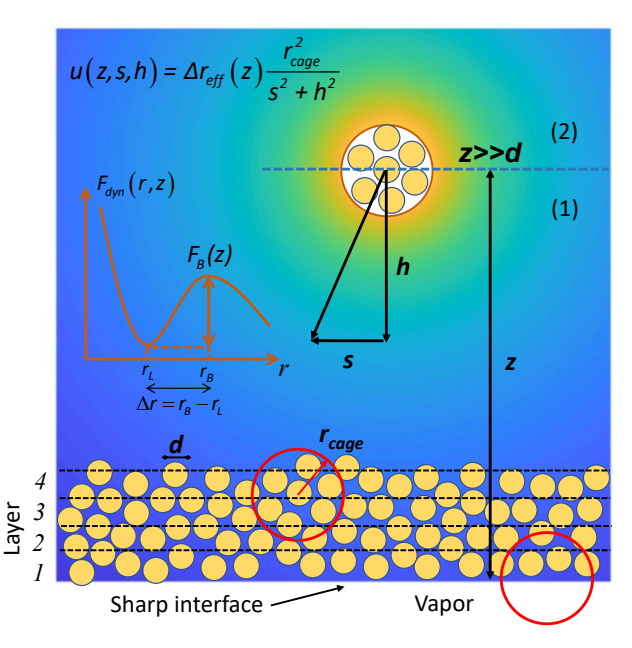


Figure 2. Schematic of the film where "layers" are shown only for illustrative reasons and density is homogeneous in all directions within the film. The regions (1) and (2) correspond to the lower and upper half space, respectively, of a hopping event characterized by the center of the cage (radius r_{cage}) located at z. The corresponding collective elastic displacement field (u) of all particles outside the cage has an amplitude set by the effective jump distance (Δr_{eff}) and depends on the defined distance variables z, h and s. The background is colored as the logarithm of $r_{cage}^2/(s^2+h^2)$ and reports on the local elastic displacement absent the gradient in $\Delta r_{eff}(z)$, with more yellow colors denoting larger displacements. The left inset in red provides a schematic illustration of the dynamic free energy as a function of tagged particle (diameter, d) displacement, r, in a liquid of density ρ . The localization length (r_L) , barrier location (r_B) , jump distance (Δr) , and local cage barrier (F_B) are defined. More details of the model and theory can be found in ref. 33 and SI.

strongly buttressed by prior results indicating a saturation (not an unbounded growth) in the range of surface gradients (or intrinsic dynamic length scale) on cooling^{26,37,41,42}.

Instead, our finding of a short-range, large-amplitude (double) exponential gradient of (alpha time) T_g followed by a lower amplitude tail suggests two distinct physical mechanisms for dynamical gradients – one medium-ranged and one long-ranged. The presence of two mechanisms for the gradient is then suggestive of two coexisting physical effects driving slow dynamics in the bulk fluid. If we specifically consider that an inverse power law describes our long-range tail data, such behavior is potentially consistent with elastic activation theories that posit that much of the dynamic activation barrier in sufficiently supercooled fragile liquids resides in a scale-free long range collective elastic field¹⁰.

More broadly, this type of two mechanism-scenario is the hallmark of the ECNLE theory, based on its two causally coupled barriers, as discussed above. The fundamental quantity in this theory is the dynamic free energy that controls particle trajectories (see Figure 2), which is constructed from knowledge of the pair structural correlations, and from which *both* barriers and the alpha relaxation time can be predicted.

ECNLE theory has been shown to capture well, often with no adjustable parameters, the temperature and density dependences of the relaxation time of diverse bulk glass-forming liquids and suspensions, including hard spheres, colloids, small molecules, and polymers^{12,13,43}, where "cooperativity" and the non-Arrhenius nature of the alpha time are dominated by the collective elastic barrier.

In the symmetry broken film (see Figure 2), both barriers in ECNLE theory depend on distance from the free surface via the z-dependence of the dynamic free energy, solely for kinetic reasons not related to any local gradient in structure or thermodynamics induced by an interface³³. Rather, the interface enters simply as a step function separating a vapor of zero density from a liquid of bulk density, ρ. The spatially heterogenous relaxation time gradient is a consequence of ^{33,44}: (i) softening of dynamic cage-scale constraints nucleated at the surface due to loss of nearest neighbors, which are transferred into the film via a layer-by-layer facilitation-like process which fully controls the local cage barrier gradient, and (ii) a gradient in the elastic barrier driven by 3 effects: (a) a z-dependent amplitude of the elastic displacement field (set by the effective jump distance, Δr_{eff}), (b) a z-dependent local elastic modulus or harmonic spring constant of the localized state (K₀) which varies as the inverse square of the dynamic localization length (r_L), and (c) geometric truncation of the elastic displacement field at the vapor interface. The local zdependent quantities Δr_{eff} and K_0 , which grow with cooling or densification, decay exponentially towards their bulk values with increasing distance from the interface with a characteristic length scale of a few particle diameters⁴⁴. Prior work focused on dynamic gradient predictions within the first ~10 particle diameters of the interface, where the theory has been shown to correctly predict the exponential decay of T_g(z) and the double exponential decay of the alpha time in the immediate vicinity of the interface, as well as spatially inhomogeneous decoupling³⁷, and factorization of the spatial and temperature dependences of the total barrier 26,33 . However, at large enough distances from the interface where F_B , Δr_{eff} and K₀ all attain their bulk values, the elastic barrier still varies with increasing z but *only* due to the cutoff of the displacement field at the vapor interface. This is the physical origin of the long-range inverse power law decay of dynamic gradients of Tg and alpha time predicted by the theory, as briefly discussed previously³³.

To better understand the predictions of ECNLE theory for the long range tail of the dynamic gradients we have carried out a new analytic analysis (with prefactors) using the same foundational hard sphere fluid model employed previously³³. As discussed above (and see Figure 2), for a relaxation event far from the interface (z>>d) the total barrier is spatially varying only due to the elastic displacement field cutoff effect. The theory predicts that the maximum amplitude of the displacement field is sufficiently small that a linear elastic analysis of its form, and hence a harmonic calculation of the corresponding elastic barrier, is valid¹². Thus, summing the elastic energy of all particles outside the cage³³ (see Figure 2 and SI for details), the contribution to the elastic barrier from the upper half-space is simply half of its bulk value,

$$F_{el}^{(2)} = 2\pi\rho \frac{K_0 \Delta r_{eff}^2}{2} r_{cage}^4 \left[\int_0^{r_{cage}} dh \int_{\frac{r_{cage}}{r_{cage}} - z^2}^{\infty} \frac{sds}{\left(s^2 + h^2\right)^2} + \int_{r_{cage}}^{\infty} dh \int_0^{\infty} \frac{sds}{\left(s^2 + h^2\right)^2} \right] = \frac{F_{el}^{bulk}}{2}, \tag{1}$$

while the contribution from the lower-half-space is reduced by the interface as:

$$F_{el}^{(1)} = 2\pi\rho \frac{K_0 \Delta r_{eff}^2}{2} r_{cage}^4 \left[\int_0^{r_{cage}} dh \int_{\sqrt{r_{cage}^2 - z^2}}^{\infty} \frac{s ds}{\left(s^2 + h^2\right)^2} + \int_{r_{cage}}^{z} dh \int_0^{\infty} \frac{s ds}{\left(s^2 + h^2\right)^2} \right] = \frac{F_{el}^{bulk}}{2} \left[1 - \frac{r_{cage}}{2z} \right]. \tag{2}$$

where F_{el}^{bulk} is the bulk elastic barrier, r_{cage} is the cage size determined from the bulk pair correlation function g(r), and the geometry variables s and h are defined in Figure 2. The subtractive term in equation (2) varies as 1/z and is a direct consequence of the cutoff of the elastic displacement field at a planar interface. Combining Eqs(1) and (2) yields

$$1 - \frac{F_{el}(z)}{F_{ol}^{bulk}} = \frac{r_{cage}}{4z} , z \gg d$$
 (3)

Per standard ECNLE theory analysis 12,33 , the mean alpha time is identified with the mean Kramer's time to cross the barrier of the z-dependent dynamic free energy including elastic barrier physics. At large z this leads analytically (see SI) to the conclusion that both the logarithm of the mean alpha time and the relative deviation in T_g obey the same inverse power law for z > d,

$$\frac{T_{g,bulk} - T_g(z)}{T_{g,bulk}} \approx \frac{F_{el}^{bulk}}{F_B^{bulk} + F_{el}^{bulk}} \frac{r_{cage}}{4z} \tag{4}$$

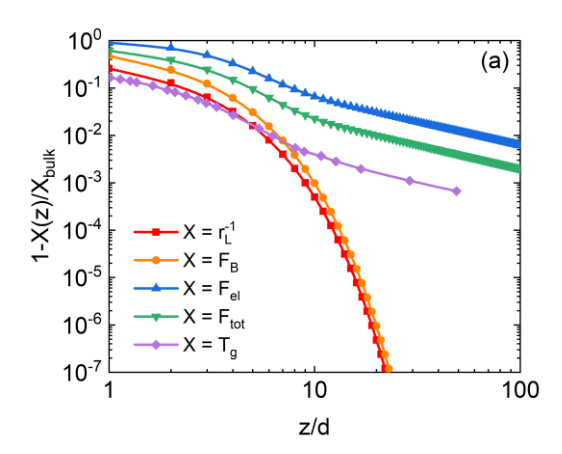
Given that prior ECNLE theory studies have shown numerically and analytically predicted³³ (well-verified in simulation^{26,39}) that the near-field gradients in the T_g deviation and $log(\tau_{\alpha}(z)/\tau_{\alpha,bulk})$ are exponential, we can now propose convenient *approximate* analytic forms for the full gradients by simply summing the predicted two asymptotic (near and far from the interface) functional forms to obtain:

$$\frac{T_{g,bulk} - T_g}{T_{g,bulk}} \approx A \exp\left(-\frac{z}{\xi}\right) + \frac{B}{z}$$
 (5)

$$\log\left(\frac{\tau_{\alpha,bulk}}{\tau_{\alpha}(z)}\right) \approx a \exp\left(-\frac{z}{\xi_{\tau}}\right) + \frac{b}{z}$$
(6)

Equations (5) and (6) do *not* represent the full ECNLE theory numerical calculations; rather they are inspired by the ECNLE analytic asymptotics, which we can employ to analyze our simulation data. As seen in Figure 1a, this form provides an excellent fit to the simulated T_g gradient data over the full z-range probed (with A, B, and ξ for the simulated $T_g(z)$ gradients equal to 0.20, 0.034 and 2.6 σ , respectively).

To buttress the above asymptotic analytic analysis we perform new, more numerically accurate, ECNLE theory calculations of the long-range gradient. These involve no fitting parameters and exhibit (as expected) a modestly more complex crossover between the low-z and high-z asymptotic regimes than described by equations (5) and (6); see the Methods section and SI for implementation details. We emphasize that no physical adjustments have been made to the prior theory in these new calculations to accommodate the new simulation data above. Rather, they involve only more precise numerical computation of the long-range tail and elastic barrier. Figures 1c and 1d explicitly show that the numerical ECNLE theory results capture the simulation findings for both the $T_g(z)$ and $\tau_{\alpha}(z)$ dynamic gradients: a short-ranged high-amplitude (double) exponential gradient for $(\tau_{\alpha}(z))$ $T_{g}(z)$ is predicted to cross over to a weak power law decay for large z. Within the modest difference in the elementary length scales d and σ (see Methods), theory and simulation are in semi-quantitative agreement for the key features of the decay: the crossover distance from exponential to power law (~ 10 segmental or bead diameters); the fractional recovery of bulk-like Tg at this crossover (~ 1.5 order of magnitude drop in Tg perturbation from the free surface), and the slowly-decaying tail in Tg. It is notable that this agreement is found despite the fact that the theory is implemented for the simple hard sphere model, thus emphasizing the semiuniversality of these gradient effects. The two-regime nature of the $T_{\rm g}$ gradient, its initial exponential



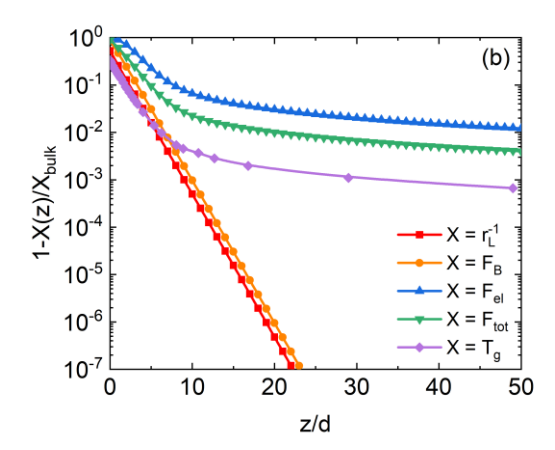


Figure 3. ECNLE theory predictions of various (normalized by the bulk) dynamic quantities as a function of dimensionless distance from the interface on a logarithmic (a) and linear (b) distance scale. Results are shown for the inverse dynamic localization length, $1/r_L$, local cage barrier, F_B , elastic barrier, F_e , total barrier, $F_{tot} = F_B + F_{eb}$ and glass transition temperature.

decay, and the power-law form and slope of the long-range tail are unambiguous signatures of the ECNLE theory physics: interface-perturbed medium-range softening of cage constraints (affects both barriers) and a longer-ranged geometric cutoff of the associated elastic displacement field. The good numerical agreement between theory and simulation provides further support for the basic physical ideas of ECNLE theory under broken symmetry film conditions.

A natural question is whether the behavior described above may qualitatively change at timescales appreciably longer than those accessible to simulations. In this regard, we recall that prior simulation, experimental, and ECNLE theory studies all have indicated that local alpha relaxation times in films obey a fractional power law decoupling relation with its bulk analog, 26,33,37,45 an important consequence of which is that T_g gradients deduced from equilibrium dynamics are relatively timescale insensitive²⁶. Indeed, as shown in Figures S3 and S4 in the SI, when the timescale convention for determination of Tg from the simulations is varied by two decades, the qualitative behavior is preserved, with a weak trend towards stronger power law tails at lower temperatures. ECNLE theory extends the analysis of this question to much longer experimental timescales. As shown in Figure 1c, the predicted Tg gradient varies only weakly as the timescale convention is changed over an enormous range from simulation to experimental timescales, and in a direction consistent with simulation. Recent experimental evidence confirms that the near-interface double-exponential relaxation time gradient persists until at least near the experimental-timescale T_g determined from a laboratory 100 s vitrification criterion, with an intrinsic dynamic decay length comparable to that reported here from simulation and theory¹⁸. While those experiments did not probe sufficiently deeply into the film to access the regime where the power-law tail reported here is expected, combined with our simulations the experiments do set bounds on the tail behavior – at simulation timescales, the power law is relatively low in magnitude and likely grows weakly on cooling; however, it is not so strong at the experimental Tg as to overwhelm the near-surface exponential (double exponential) gradient of $T_{\rm g}$ (relaxation time).

The experimental impacts of the long-range tail we report will be difficult to resolve in most mean-film-property measurements. The most sensitive of these measurements have provided some insight into the distribution of relaxation times within the film, such as dielectric spectroscopy measurements reporting on broadening of the mean relaxation process in films relative to bulk⁴⁶. These experiments point to the

presence of a domain of faster dynamics near the surface, but the observed broadening is dominated by the short range double-exponential gradient in τ_{α} . The effect of the long range contribution to the gradient would be within the extreme tail of this film-averaged distribution, and whether the long-range gradient tail could be extracted or inferred from film-averaged data will require future quantitative theoretical analysis. We believe the experimental prospects are challenging given practical uncertainties and convolution with the bulk breadth of the relaxation process. Similarly, experiments that employ optical photobleaching have pointed to the presence of two relaxation processes in the film below Tg, with one attributed to surface relaxation and one to bulk-like relaxation⁴⁷. This behavior (and also broadening of the film-averaged frequency-domain dielectric loss) has been previously predicted by the ECNLE theory⁴⁸. However, it is dominated within the theory by the steep near surface double-exponential gradient of the alpha time relaxation time and is likely not a good target for experimental observation of the long-ranged tail. One possible whole-film target for observation of these effects may be in intermediate-thickness films, where the spatially long range tail can compensate for its relatively low magnitude resulting in an appreciable contribution to the overall shift in relaxation time or Tg. Indeed, this long range tail is likely responsible for our recent simulation report of excess accelerations in dynamics in intermediate films relative to what would be expected from exponential gradients alone³⁹.

Concerning the ECNLE theory predictions on the 100 s timescale of the glass transition temperature gradient in Figure 1d, the quantitative results suggest that direct spatially-resolved experimental observation of the power law tail in T_g would require sub-Kelvin sensitivity to T_g shifts, which would likely be extraordinarily challenging in conjunction with the demand for spatial resolution. More promisingly, observing the long-range tail in the relaxation time spatial gradient would require sufficient sensitivity to detect timescale shifts of order 10% to 60% - relatively tractable from a sensitivity standpoint. However, the demand that these measurements be spatially-resolved out to distances of several 10's of nm from the interface will require new advances in spatially resolved measurements near interfaces to extend further into the material 18,49,50 .

Importantly, ECNLE theory also predicts how the amplitude of the power-law tail varies with chemistry, and for the *same* physical reason it predicts a modest dependence on vitrification timescale criterion. Within the theory, the relative magnitude of collective elastic to local cage barriers at T_g is *nonuniversal*, and directly related to the bulk dynamic fragility⁵¹ (see also SI). Liquids with a weaker relative contribution from collective elasticity (e.g., strong glass formers) are predicted to exhibit a weaker long-range power law tail in their interfacial dynamics gradient (see SI). This provides an additional testable prediction for future simulations and experiments possessing sufficient sensitivity to resolve the dynamic gradient tail. The question of the dependence of perturbed surface dynamics on materials chemistry has long been a focus of the field for both practical and fundamental reasons, and very recent experimental results have indeed suggested a strong dependence of these perturbations on the bulk liquid dynamic fragility^{52,53}.

To conclude, the discovery of a long range, apparently scale-free dynamical gradient induced by a single interface suggests that low-magnitude interfacial perturbations to T_g and dynamics in nanostructured materials can persist over a remarkably long range. Indeed, a 1/z power law tail in $T_g(z)$ and $\tau_\alpha(z)$ formally has an infinite range (divergent zeroth and first moments), which based on our theoretical analysis is not expected to change at an ultra large distance from the interface. Our findings may provide a theoretical starting point for understanding the puzzling observation of exceptionally long range interfacial perturbations of T_g in a variety of experimental systems, including polymeric bilayer films^{54,55}. Fundamentally, our core simulation findings provide a new *direct* validation of a signature foundational

prediction of ECNLE theory – that collective elasticity plays a critical role in structural relaxation in deeply supercooled liquids. This provides further support for this approach which has successfully addressed other diverse glassy phenomena including: nanoconfinement effects on equilibrium dynamics over a large range of film thicknesses³⁹; the temperature and density dependences of the bulk alpha relaxation time in a large range of polymers⁴³, small molecules¹³, and colloidal glass formers¹²; the emergence of diffusion-relaxation decoupling in deeply supercooled liquids⁵¹; and a non-causal relationship between thermodynamics and dynamics in molecular, polymer and inorganic glass forming liquids⁵⁶.

Acknowledgements

DSS and AG were supported by the National Science Foundation (NSF) CAREER Award under Grant No. DMR - 1849594.

Author Contributions Statement

The manuscript and SI were written based on the contributions of all authors. AG performed all simulations under DSS' supervision. AG and DSS jointly conceived of and analyzed all simulations. AP and KS performed all ECNLE theory analytic analysis and numerical calculations.

Competing Interests Statement

The authors declare no competing interests.

Supplementary Information

Supplementary simulation methods, data, and additional theoretical analysis and calculations are available in the supplementary PDF. Average (across 3 runs) temperature and position dependent relaxation times, and average relaxation times, and associated standard deviations, are available in the supplementary excel data file.

References

- 1. Cavagna, A. Supercooled liquids for pedestrians. Phys. Rep.-Rev. Sec. Phys. Lett. 476, 51–124 (2009).
- 2. Debenedetti, P. G. & Stillinger, F. H. Supercooled liquids and the glass transition. *Nature* **410**, 259–267 (2001).
- 3. Angell, C. A. Formation of Glasses from Liquids and Biopolymers. Science 267, 1924–1935 (1995).
- 4. Adam, G. & Gibbs, J. H. On the Temperature Dependence of Cooperative Relaxation Properties in Glass-Forming Liquids. *J. Chem. Phys.* **43**, 139–146 (1965).
- 5. Kirkpatrick, T. R., Thirumalai, D. & Wolynes, P. G. Scaling concepts for the dynamics of viscous liquids near an ideal glassy state. *Phys. Rev. A* **40**, 1045–1054 (1989).

- 6. Lubchenko, V. & Wolynes, P. G. Theory of Structural Glasses and Supercooled Liquids. *Annual Review of Physical Chemistry* **58**, 235–266 (2007).
- 7. White, R. P. & Lipson, J. E. Polymer Free Volume and Its Connection to the Glass Transition.

 Macromolecules 49, 3987–4007 (2016).
- 8. Long, D. & Lequeux, F. Heterogeneous dynamics at the glass transition in van der Waals liquids, in the bulk and in thin films. *Eur. Phys. J. E* **4**, 371–387 (2001).
- 9. Chandler, D. & Garrahan, J. P. Dynamics on the Way to Forming Glass: Bubbles in Space-Time. *Annual Review of Physical Chemistry* **61**, 191–217 (2010).
- 10. Dyre, J. C. Colloquium: The glass transition and elastic models of glass-forming liquids. *Reviews of Modern Physics* **78**, 953–972 (2006).
- 11. Hall, R. W. & Wolynes, P. G. The aperiodic crystal picture and free-energy barriers in glasses. *Journal of Chemical Physics* **86**, 2943–2948 (1987).
- 12. Mirigian, S. & Schweizer, K. S. Elastically cooperative activated barrier hopping theory of relaxation in viscous fluids. I. General formulation and application to hard sphere fluids. *J. Chem. Phys.* **140**, 194506 (2014).
- 13. Mirigian, S. & Schweizer, K. S. Elastically cooperative activated barrier hopping theory of relaxation in viscous fluids. II. Thermal liquids. *J. Chem. Phys.* **140**, 194507 (2014).
- 14. Forrest, J. A. & Dalnoki-Veress, K. The glass transition in thin polymer films. *Advances in Colloid* and *Interface Science* **94**, 167–195 (2001).
- 15. Alcoutlabi, M. & McKenna, G. B. Effects of confinement on material behaviour at the nanometre size scale. *Journal of Physics: Condensed Matter* **17**, R461–R524 (2005).
- Baschnagel, J. & Varnik, F. Computer simulations of supercooled polymer melts in the bulk and in confined geometry. *Journal of Physics: Condensed Matter* 17, R851–R953 (2005).

- 17. Ediger, M. D. & Forrest, J. A. Dynamics near Free Surfaces and the Glass Transition in Thin Polymer Films: A View to the Future. *Macromolecules* **47**, 471–478 (2014).
- 18. Li, Y. *et al.* Surface diffusion in glasses of rod-like molecules posaconazole and itraconazole: effect of interfacial molecular alignment and bulk penetration. *Soft Matter* **16**, 5062–5070 (2020).
- 19. Ediger, M. D. Perspective: Highly stable vapor-deposited glasses. *J. Chem. Phys.* **147**, 210901 (2017).
- 20. Simmons, D. S. An Emerging Unified View of Dynamic Interphases in Polymers. *Macromol. Chem. Phys.* **217**, 137–148 (2016).
- 21. Keddie, J. L., Jones, R. A. L. & Cory, R. A. Size-Dependent Depression of the Glass Transition Temperature in Polymer Films. *Europhysics Letters (EPL)* **27**, 59–64 (1994).
- 22. Jancar, J. *et al.* Current issues in research on structure-property relationships in polymer nanocomposites. *Polymer* **51**, 3321–3343 (2010).
- 23. Christie, D., Register, R. A. & Priestley, R. D. Direct Measurement of the Local Glass Transition in Self-Assembled Copolymers with Nanometer Resolution. *ACS Cent. Sci.* **4**, 504–511 (2018).
- 24. Wunderlich, B. Reversible crystallization and the rigid-amorphous phase in semicrystalline macromolecules. *Prog. Polym. Sci.* **28**, 383–450 (2003).
- 25. Jackson, C. L. & McKenna, G. B. The glass transition of organic liquids confined to small pores. *Journal of Non-Crystalline Solids* **131–133**, Part **1**, 221–224 (1991).
- 26. Schweizer, K. S. & Simmons, D. S. Progress towards a phenomenological picture and theoretical understanding of glassy dynamics and vitrification near interfaces and under nanoconfinement. *Journal of Chemical Physics* **151**, 240901 (2019).
- 27. Richert, R. Dynamics of Nanoconfined Supercooled Liquids. *Annual Review of Physical Chemistry* **62**, 65–84 (2011).

- 28. Napolitano, S., Glynos, E. & Tito, N. B. Glass transition of polymers in bulk, confined geometries, and near interfaces. *Rep. Prog. Phys.* **80**, 036602 (2017).
- 29. Stevenson, J. D. & Wolynes, P. G. On the surface of glasses. J Chem Phys 129, 234514 (2008).
- 30. Merabia, S., Sotta, P. & Long, D. Heterogeneous nature of the dynamics and glass transition in thin polymer films. *Eur. Phys. J. E* **15**, 189–210 (2004).
- 31. White, R. P. & Lipson, J. E. G. Dynamics across a Free Surface Reflect Interplay between Density and Cooperative Length: Application to Polystyrene. *Macromolecules* **54**, 4136–4144 (2021).
- 32. Salez, T., Salez, J., Dalnoki-Veress, K., Raphaël, E. & Forrest, J. A. Cooperative strings and glassy interfaces. *Proceedings of the National Academy of Sciences of the United States of America* **112**, 8227 (2015).
- 33. Phan, A. D. & Schweizer, K. S. Influence of Longer Range Transfer of Vapor Interface Modified Caging Constraints on the Spatially Heterogeneous Dynamics of Glass-Forming Liquids.

 Macromolecules 52, 5192–5206 (2019).
- 34. Mangalara, J. H., Marvin, M. D., Wiener, N. R., Mackura, M. E. & Simmons, D. S. Does fragility of glass formation determine the strength of Tg-nanoconfinement effects? *The Journal of Chemical Physics* **146**, 104902 (2017).
- 35. Paul Z. Hanakata, Jack F. Douglas, & Francis W. Starr. Local Variation of Fragility and Glass Transition Temperature of Ultra-thin Supported Polymer Films. *Journal of Chemical Physics* **137**, 244901 (2012).
- 36. Zhou, Y. & Milner, S. T. Short-Time Dynamics Reveals Tg Suppression in Simulated Polystyrene Thin Films. *Macromolecules* **50**, 5599–5610 (2017).
- 37. Diaz-Vela, D., Hung, J.-H. & Simmons, D. S. Temperature-Independent Rescaling of the Local Activation Barrier Drives Free Surface Nanoconfinement Effects on Segmental-Scale Translational Dynamics near Tg. *ACS Macro Lett.* 1295–1301 (2018) doi:10.1021/acsmacrolett.8b00695.

- 38. Scheidler, P., Kob, W. & Binder, K. Cooperative motion and growing length scales in supercooled confined liquids. *Europhysics Letters (EPL)* **59**, 701–707 (2002).
- 39. Ghanekarade, A., Phan, A. D., Schweizer, K. S. & Simmons, D. S. Nature of dynamic gradients, glass formation, and collective effects in ultrathin freestanding films. *PNAS* **118**, e2104398118 (2021).
- 40. Schmidtke, B., Hofmann, M., Lichtinger, A. & Rössler, E. A. Temperature Dependence of the Segmental Relaxation Time of Polymers Revisited. *Macromolecules* **48**, 3005–3013 (2015).
- 41. Kob, W., Roldán-Vargas, S. & Berthier, L. Non-monotonic temperature evolution of dynamic correlations in glass-forming liquids. *Nature Physics* **8**, 164–167 (2012).
- 42. Hocky, G. M., Berthier, L., Kob, W. & Reichman, D. R. Crossovers in the dynamics of supercooled liquids probed by an amorphous wall. *Phys. Rev. E* **89**, 052311 (2014).
- 43. Mirigian, S. & Schweizer, K. S. Dynamical Theory of Segmental Relaxation and Emergent Elasticity in Supercooled Polymer Melts. *Macromolecules* **48**, 1901–1913 (2015).
- 44. Phan, A. D. & Schweizer, K. S. Theory of the spatial transfer of interface-nucleated changes of dynamical constraints and its consequences in glass-forming films. *J. Chem. Phys.* **150**, 044508 (2019).
- 45. White, R. P. & Lipson, J. E. G. To Understand Film Dynamics Look to the Bulk. *Phys. Rev. Lett.* **125**, 058002 (2020).
- 46. Napolitano, S. & Wübbenhorst, M. Structural relaxation and dynamic fragility of freely standing polymer films. *Polymer* **51**, 5309–5312 (2010).
- 47. Paeng, K., Swallen, S. F. & Ediger, M. D. Direct Measurement of Molecular Motion in Freestanding Polystyrene Thin Films. *J. Am. Chem. Soc.* **133**, 8444–8447 (2011).
- 48. Mirigian, S. & Schweizer, K. S. Theory of activated glassy relaxation, mobility gradients, surface diffusion, and vitrification in free standing thin films. *The Journal of Chemical Physics* **143**, 244705 (2015).

- 49. Chowdhury, M. *et al.* Spatially Distributed Rheological Properties in Confined Polymers by Noncontact Shear. *J. Phys. Chem. Lett.* 1229–1234 (2017) doi:10.1021/acs.jpclett.7b00214.
- 50. Hao, Z. *et al.* Mobility gradients yield rubbery surfaces on top of polymer glasses. *Nature* **596**, 372–376 (2021).
- 51. Xie, S.-J. & Schweizer, K. S. A collective elastic fluctuation mechanism for decoupling and stretched relaxation in glassy colloidal and molecular liquids. *J. Chem. Phys.* **152**, 034502 (2020).
- 52. Li, Y. et al. Surface Diffusion Is Controlled by Bulk Fragility across All Glass Types. *Phys. Rev. Lett.*128, 075501 (2022).
- 53. Evans, C. M., Deng, H., Jager, W. F. & Torkelson, J. M. Fragility is a Key Parameter in Determining the Magnitude of Tg-Confinement Effects in Polymer Films. *Macromolecules* **46**, 6091–6103 (2013).
- 54. Baglay, R. R. & Roth, C. B. Communication: Experimentally determined profile of local glass transition temperature across a glassy-rubbery polymer interface with a Tg difference of 80 K. *The Journal of Chemical Physics* **143**, 111101 (2015).
- 55. Huang, X. & Roth, C. B. Optimizing the Grafting Density of Tethered Chains to Alter the Local Glass

 Transition Temperature of Polystyrene near Silica Substrates: The Advantage of Mushrooms over

 Brushes. ACS Macro Lett. 7, 269–274 (2018).
- 56. Mei, B., Zhou, Y. & Schweizer, K. S. Experimental test of a predicted dynamics–structure–thermodynamics connection in molecularly complex glass-forming liquids. *PNAS* **118**, (2021).
- 57. Grest, G. & Kremer, K. Molecular-Dynamics Simulation for Polymers in the Presence of a Heat Bath. *Phys. Rev. A* **33**, 3628–3631 (1986).
- 58. Mackura, M. E. & Simmons, D. S. Enhancing heterogenous crystallization resistance in a bead-spring polymer model by modifying bond length. *Journal of Polymer Science Part B: Polymer Physics* **52**, 134–140 (2014).

- 59. Ivancic, R. J. S. & Riggleman, R. A. Dynamic phase transitions in freestanding polymer thin films. *PNAS* **117**, 25407–25413 (2020).
- 60. Vogel, H. Das temperatur-abhängigkeitsgesetz der viskosität von flüssigkeiten. *Phys. Zeit.* **22**, 645–646 (1921).
- 61. Fulcher, G. S. Analysis of recent measurements of the viscosity of glasses. *J. Am. Ceram. Soc.* **8**, 339 (1925).

Methods

Details of the simulations, which employ a bead-spring polymer model⁵⁷ modified to exhibit exceptional crystallization resistance⁵⁸, are provided in the SI. Simulated films, which are approximately 50 segmental (bead) diameters (σ, approximately 1 nm) thick and comparably wide (~40 x 40 σ), are supported on a nearly dynamically neutral substrate such that dynamical perturbations in the film are dominated only by a single free surface. Films are supported on a substrate with a substrate-polymer pairwise interaction strength that is tuned to be 51.1% of the polymer-polymer bead interaction strength, which yields almost no local gradient in dynamics (see SI Figure 1). As compared to the large literature of molecular simulations of two-interface freestanding films^{16,26,59}, this allows for quantification of altered dynamics much further from the dynamically active free surface without interference by a second surface gradient - up to at least 35 σ (about 35 nm) from the free surface. Corresponding bulk relaxation times at the lowest temperatures simulated approach 10^5 LJ time units τ_{LJ} (about 100 ns). We compute $T_g(z)$ by fitting the temperature dependence of the relaxation time $\tau_{\alpha}(z)$ at each position z and then defining their $T_{g}(z)$ as the temperature at which the local relaxation time is 10⁵ Lennard Jones time units. We perform this fit using two very different widely employed empirical functional forms – the Vogel-Fulcher Tammann equation 60,61 (results shown in SI) and the Cooperative Model of Schmidtke et al.40 - to ensure that the results are not a consequence of the choice of fit form. Three replicas of this simulation and of the corresponding bulk system are simulated, and error bars are propagated from these replicas. Together with averaging over multiple runs, this protocol provides sufficient range and sufficient statistical power to resolve the longrange form of the gradient in glass transition temperature emanating from a free surface.

In order to numerically compute $T_g(z)$ gradients from ECNLE theory, we adopt a well-established method^{12,37} to map the hard sphere model to a typical fragile liquid (polystyrene)⁴³ at 1 atm (additional details in SI). We also present numerical relaxation time gradient calculations which are *not* tied to the polystyrene mapping. For the simulated flexible polymer bead-spring model, the elementary length scale σ is expected to be of order, but modestly smaller than, the hard-sphere theory diameter d based on the mapping procedure for polymers⁴³ and prior simulation-theory studies³⁹.

Data Availability Statement

All relevant data are included in the paper and/or its supplementary information files. Raw simulation trajectory files, which are prohibitively large, are available upon reasonable request from DSS.

Code Availability Statement

All results in this manuscript employed openly available codes and/or standard numerical algorithms.